



# Experimental investigation on the behavior of fly-ash based geopolymer reinforced concrete beams strengthened with CFRP

Ahmed S. Eisa<sup>a</sup>, Mostafa H. Ahmed<sup>a, \*\*</sup>, Ivo Demjan<sup>b</sup>, Dušan Katunský<sup>c, \*</sup>

<sup>a</sup> Department of Structural Engineering, Faculty of Engineering, Zagazig University, Zagazig, 44511, Egypt

<sup>b</sup> Institute of Structural Engineering and Transportation Structures, Faculty of Civil Engineering, Technical University of Košice, Slovakia

<sup>c</sup> Institute of Architectural Engineering, Faculty of Civil Engineering, Technical University of Košice, Slovakia

## ARTICLE INFO

### Keywords:

Fly-ash  
Geopolymer concrete  
Alkaline activator  
Flexural strengthening  
Shear strengthening  
Ultimate capacity load  
CFRP sheet  
Ductility index.)

## ABSTRACT

Recently, the demand for strengthening and rehabilitation of existing RC structures has increased due to the corrosion of internal steel reinforcement, variations in temperature, and increasing loading. As a result, several experimental studies have been performed to investigate the structural behaviour of strengthening RC beams with CFRP sheets, but few for GPC beams; therefore, this investigation focuses on the behaviour of strengthening GPC beams with CFRP sheets. In this experimental work, a set of ten specimen beams with the same cross section of 100 × 250 mm and 850 mm length with a 750 mm clear span were cast in two groups of five beams each. First group (flexural group) to study the flexural behavior, and the second one for the shear behaviour (shear group). In each group, the first beam was carried out as an RC control beam and the second as a GPC control beam without strengthening, while the other three beams were cast as GPC beams and strengthened with various schemes of CFRP sheets. All specimens were tested up to failure under two-sided static loading (four-point bending). The first cracking, yielding, and ultimate failure loads, the deflection values at midspan, the longitudinal bar strain, and the concrete strain were recorded for all tested specimens. The experimental results indicated that the Flexural Strengthening of GPC with CFRP sheet increased the First Cracking, yield and ultimate load capacity by 25.33%, 15.3% and 15% respectively, as well as, deflection was decreased by 16% on average while ductility and toughness have improved by 10% and 12% on average compared to R.C Beam. On the other side, the Shear Strengthening of GPC with CFRP strips increased the First Cracking, yield and ultimate load by 43%, 70% and 68% respectively, as well as, shear ductility has improved by 8% on average compared to R.C Beam. Overall, the different schemes of externally bound CFRP sheets have improved the flexural and shear behaviour of GPC beams.

## 1. Introduction

In the last century, the demand for concrete has increased daily to keep up with the development in the construction field, and so has the production of ordinary Portland cement (OPC), the leading material for the concrete industry. Portland cement-based concrete has become the second most widely used material worldwide after water, and it was expected that the global annual cement production would be 5.9 billion tons in 2020 [1]. Moreover, it's increased by 10% every year [2]. The massive production of Ordinary

\* Corresponding author.

\*\* Corresponding author.

E-mail addresses: [mou.hassan@eng.zu.edu.eg](mailto:mou.hassan@eng.zu.edu.eg) (M.H. Ahmed), [dušan.katunský@tuke.sk](mailto:dušan.katunský@tuke.sk) (D. Katunský).

<https://doi.org/10.1016/j.heliyon.2023.e17674>

Received 3 March 2023; Received in revised form 29 May 2023; Accepted 25 June 2023

Available online 26 June 2023

2405-8440/© 2023 Published by Elsevier Ltd.

This is an open access article under the CC BY-NC-ND license

(<http://creativecommons.org/licenses/by-nc-nd/4.0/>).

Portland Cement OPC, which consumes a lot of energy and natural resources, emits a lot of carbon dioxide CO<sub>2</sub> into the atmosphere. It has been discovered that producing 1 ton of OPC requires approximately 2 ton of raw materials such as shale and limestone and emits approximately one ton of CO<sub>2</sub>. Furthermore, the cement industry emits approximately 7% of total greenhouse gas emissions GHGs that cause global warming [3–5]. CO<sub>2</sub> is one of the GHGs responsible for approximately 65% of global warming [6,7]. Simply put, the more OPC produced, the more CO<sub>2</sub> emissions there will be, as well as the decay of confined natural resources [8,9]. Therefore, researchers around the world do their best to find an alternative binder material to replace OPC and produce eco-friendly concrete.

A new eco-friendly, sustainable, durable, and cost-effective material called “geopolymer” has attracted attention as an alternative binder to reduce the production of OPC. It was first used by Davidovits in 1970 [10]. Geopolymer binder is a new inorganic polymeric system of aluminosilicates that was formed by using silica and alumina that are available in clay (metakaolin) [11]. Geopolymer binder is the result of a reaction between solid aluminosilicate powder and alkaline activator solutions. It has structural strength from the polycondensation of alumina and silica precursors with a high content of alkali activator [12]. According to the presence of calcium, the precursor materials are classified into two groups: low calcium and high calcium [13]. Low calcium precursors include fly-ash Class F, silica fume (SF), metakaolin (MK), red mud (RM), and rice husk ash (RHA), while high calcium precursors include fly-ash Class C and ground granulated blast furnace slag (GGBFS) [13]. The low-calcium fly ash has silicon and aluminium oxides that react with the alkaline solution to form the geopolymer paste, which binds fine and coarse aggregates as well as other unreacted components together to form the geopolymer concrete [14].

Geopolymer concrete GPC is a new generation in the construction industry. It has significant benefits, such as reducing the emission of global warming gases and using industrial waste for the production of concrete [15]. The utilisation of GPC has reduced the emission of CO<sub>2</sub> by 80–90% compared to that of OPC concrete [16]. In addition, GPC has recently gained popularity among all binder materials due to its effective cost, excellent durability, good resistance to chemicals and fire, low permeability, low thermal conductivity, less energy consumption, eco-friendliness, as well as earlier compressive strength [17–21]. Therefore, GPC has proven its efficiency to be a better alternative to OPC concrete. Among precursor materials, fly ash is the most popular source material that is used to produce GPC [4,14,22]. The utilisation of low-calcium fly ash-based GPC was recommended as a replacement for OPC concrete because it performed better and had fewer environmental disasters [2]. Fly-ash-based GPC shows many advantages. Compared to OPC concrete, low-calcium fly ash-based GPC has excellent compressive strength, significant resistance to chemicals and acid attacks, suffers very little shrinkage, and has low creep [7].

Several researchers have studied the structural behaviour of GPC. It is determined by the bond between the concrete element composition and the embedded length of steel bars [14]. It was found that when fly-ash-based GPC beams were subjected to flexure loading, they behaved similarly to OPC beams in terms of first cracking load, cracking width and length, load deflection curves, stiffness, failure mode, and ultimate failure load [23,24]. Beam effective depth (*d*), shear span to depth ratio (*a/d*) [25], support conditions, longitudinal [26], and transverse reinforcement ratio [27] are the main parameters that affected the shear capacity of GPC beams. Sharmila [25] investigated the shear strength of fly ash-based GPC beams with various ratios of *a/d* and found that the inclined angle of the diagonal crack varied with *a/d* values for all beams and the load deflection curve was almost linear for lower *a/d* ratios. Chang [26] studied the shear capacity of fly ash-based GPC beams with various ratios of longitudinal reinforcement and found that the shear capacity of the beams was affected by the longitudinal reinforcement ratio and increased with it.

Recently, the need to strengthen and rehab existing RC structures has increased due to corrosion of internal steel reinforcement, variations in temperature, and increasing loading. Several experimental and numerical studies were carried out to study the structural behaviour of RC members strengthened with FRP materials. Among different types of FRP composite materials, CFRP is the most popular and applicable for strengthening RC structures due to its numerous advantages, including high strength compared to its weight, durability, versatility, flexibility in application techniques, ease of handling and installation, high fatigue property, and low thermal conductivity [28]. For strengthening beams with CFRP, several studies were carried out for RC beams but little for GPC beams. Sherwin [29] investigated the flexural strength of GPC beams strengthened with CFRP sheet and compared them with the control GPC



Fig. 1. (a) Fly-ash. (b) Sodium hydroxide. (c) Liquid Sodium Silicate.

beams. They found that the first cracking load, service load, yield, and ultimate load were higher compared to GPC control beams, and that the failure modes and crack pattern were less severe compared to GPC control beams.

## 2. Experimental program

### 2.1. Material used

Two sizes of crushed gravel (dolomite) were used with maximum nominal diameters of 9.2 mm and 18 mm and a specific gravity of 2.7. Dolomite was used as an alternative for gravel due to its coarser and more irregular surfaces, as well as its high surface area-to-volume ratio. The aggregate was washed with water before use to reduce the wastage of mixing water and allowed to dry at room temperature. It was then kept in stocks so that there would be no change in their properties as a result of vibration.

Natural and clean sand with a maximum nominal size of 4.6 mm and a fineness modulus of 2.77 was used as fine aggregate for all mixes. It was free of impurities, silt, clay, and inorganic compounds, as well as washed before usage and dried at room temperature. To achieve the desired consistency of the concrete mixture, sand accounted for 0.35 by weight of the total aggregate and dolomite accounted for 0.65 by weight of the total aggregate in all concrete mixes.

Low-calcium fly-ash class (F) was used in this investigation, as shown in Fig. 1a. It has a grey color, a fine powder texture, and spherical particles as well as a lubricating effect that improves the flow and pumping of concrete while reducing the amount of water required. It was brought from SIKA Egypt, for a construction chemicals company as provided by manufacturer's datasheet [30] and according to ASTM 618-19 [31], as shown in Fig. 1a. Table 1 displays the physical and chemical properties of fly ash as determined by the Zagazig University faculty of science laboratory.

Alkali activator solution is a mixture of two chemical components Sodium hydroxide (SH) and Liquid Sodium Silicate (LSS) as shown in Fig. 1b & c. The Sodium hydroxide NaOH was used as pellets, of 490 gm in 1 L, which can be dissolved into water to have the required molarity of 12 M and 98% purity of NaOH. The second one was Liquid Sodium Silicate  $\text{Na}_2\text{SiO}_3$  which had 34.64%, 16.27% and 49.09% of SiO, Na<sub>2</sub>O and water respectively by weight. Sodium hydroxide solution was mixed with Liquid Sodium Silicate immediately before casting of all specimens to have the required alkaline activators. Table 2 shows the chemical properties of Sodium hydroxide and Liquid Sodium Silicate that was tested in zagazig univeristy laboratories.

The carbon fabric that is used in the strengthening of the GPC beams is commercially known as SikaWrap® 230C and was brought from the SIKA Egypt company, as shown in Fig. 2a. It's a uniaxially woven CF fabric with mid-range strength that can be installed using both dry and wet application methods. Table 3 shows the mechanical properties of the carbon fabric that was obtained by the manufacturer and used in this research.

Sikadur® 330 is a two-component system comprised of a white thixotropic epoxy-based impregnating resin and a grey adhesive. They are combined to form a light grey paste (resin part A and hardener part B are weighted at 4:1). Sikadur® 330 was brought from the SIKA Egypt company and used for SikaWrap® fabric installation using the dry application technique. Table 3 shows the mechanical properties of the impregnation resin that was obtained by the manufacturer.

### 2.2. Specimens details and preparations

In this experimental work, a set of ten tested beams with the same cross section of 100x250 mm and 850 mm length with a 750 mm clear span were cast, and the ratio between shear span and depth (a/d) was equal to 1. All specimens were tested up to failure under two-sided symmetric static loading (four-point bending) as shown in Fig. 3. All the tested beams consisted of two groups of five beams each. The first group (flexural group) had 2  $\phi$  10 lower reinforcement, 2  $\phi$  8 upper reinforcement, and 8  $\phi$  8 stirrups, as shown in Fig. 4. The second group, to study shear behaviour (shear group), had 2  $\phi$  12 lower reinforcement, 2  $\phi$  10 upper reinforcement, and 3  $\phi$  8 stirrups, as shown in Fig. 5. For all tested beams, the deflection and longitudinal steel strain were measured at the mid-span of beams, as well as the surface strain at the top and bottom faces of beams, using concrete strain gauges. Table 4 describes the experimental programme and the strengthening schemes of GPC beams with CFRP sheets in shear and flexural. Fig. 6(a,b and c) show the Flexural strengthening schemes with CFRP sheets while Fig. 7(a,b and c) show the shear strengthening schemes with CFRP strips.

**Table 1**

The properties of Fly ash, that used in this research.

Fly-Ash			
Physical Property	Measured Value	Chemical Property	Measured Value (%)
color	Grey (Blackish)	SiO <sub>2</sub>	57.3
specific gravity	2.62	CaO	1.34
		Al <sub>2</sub> O <sub>3</sub>	30.8
		Fe <sub>2</sub> O <sub>3</sub>	5.02
		Na <sub>2</sub> O	0.08
		SO <sub>3</sub>	0.05
		MgO	0.95
		K <sub>2</sub> O	1.05
		LOI	0.8
		Cl	0.04

**Table 2**  
Chemical properties of NaOH and Na<sub>2</sub>SiO<sub>3</sub>.

Sodium hydroxide NaOH		Sodium Silicate Na <sub>2</sub> SiO <sub>3</sub>	
Chemical Property	Value	Chemical Property	Value
Dry fabric density	1.82 g/cm <sup>3</sup>	Dry density	1.3 ± 0.1 kg/L
Dry fabric thickness	0.129 mm	Tensile Strength	30 MPa
Dry Tensile Strength	4000 MPa	Elastic modulus in flexural	3800 MPa
Modulus of Elasticity	230 GPa	Elastic modulus in tension	4500 MPa
Elongation at Break	1.80%	Elongation at Break	0.7%

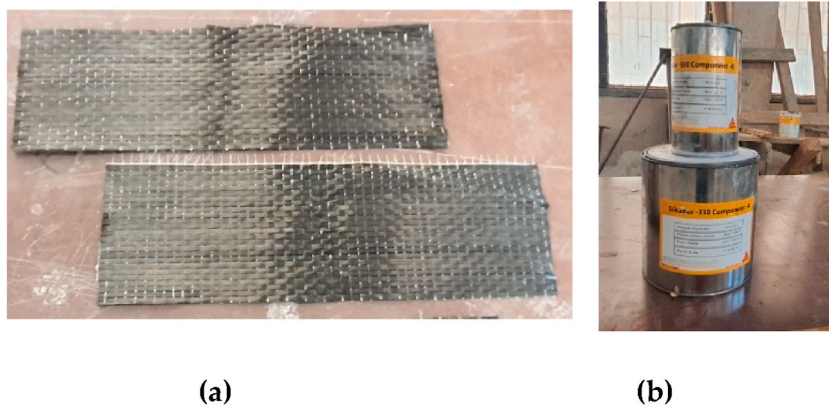


**Fig. 2.** (a) Carbon fiber. (b) Sikadur® –330 (Impregnation resin).

**Table 3**  
The mechanical properties of carbon fabric and Sikadur® –330 (Impregnation resin).

Carbon fabric		Sikadur® –330	
Property	Value	Property	Value
Dry fabric density	1.82 g/cm <sup>3</sup>	Dry density	1.3 ± 0.1 kg/L
Dry fabric thickness	0.129 mm	Tensile Strength	30 MPa
Dry Tensile Strength	4000 MPa	Elastic modulus in flexural	3800 MPa
Modulus of Elasticity	230 GPa	Elastic modulus in tension	4500 MPa
Elongation at Break	1.80%	Elongation at Break	0.7%

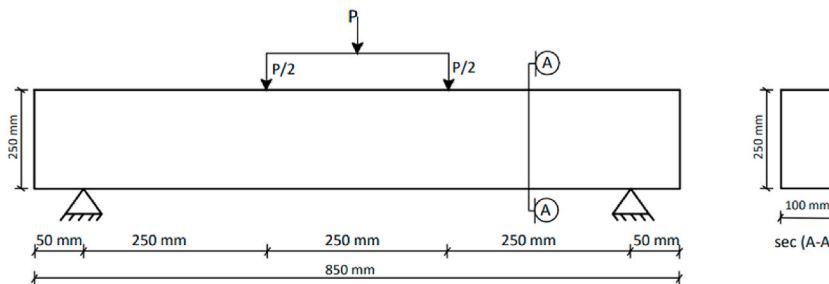


**Fig. 3.** Beams dimensions and loading system.

According to several studies [32,33], it has been found that the molarity of sodium hydroxide ranged from 8 M to 16 M, the alkali to fly ash ratio ranged from 0.25 to 0.75, and the ratio of liquid sodium silicate Na<sub>2</sub>SiO<sub>3</sub> to sodium hydroxide NaOH ranged from 0.17 to 3. It was also reported [34] that for good strength properties in geopolymer concrete, the Na<sub>2</sub>SiO<sub>3</sub> to NaOH ratio should be 2.5, the alkali to fly ash ratio should be 0.55, and the water to geopolymer solid ratio should be 0.25. Therefore, 12 standard cubes with 150 × 150 × 150 mm side lengths were cast and tested at the age of 28 days as trial mixes to determine the compressive and splitting tensile strengths of geopolymer concrete according to ASTM C109 [35] and ASTM C496 [36], respectively. Table 5 shows mixture proportions for 1 m<sup>3</sup> of RC control beam and mixture proportions for 1 m<sup>3</sup> of GPC beams.

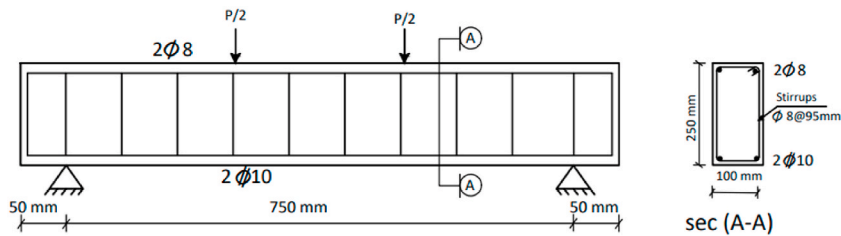


Fig. 4. Beams reinforcement details for flexural group.

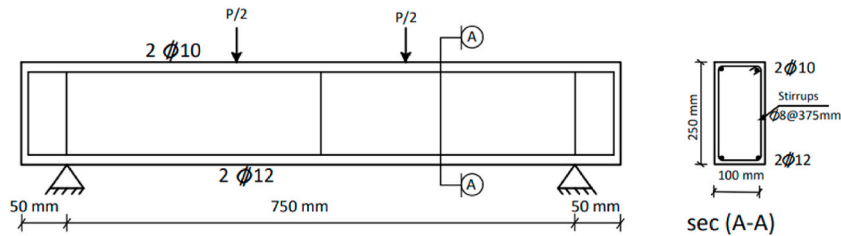


Fig. 5. Beams reinforcement details for shear group.

Table 4

The strengthening schemes of CFRP in flexural and shear groups of tested beams.

Flexural Group		Shear Group	
<b>BF1</b>	Reinforced Concrete RC control beam without strengthening	<b>BS1</b>	Reinforced Concrete RC control beam without strengthening
<b>BF2</b>	Geopolymer Concrete GC control beam without strengthening	<b>BS2</b>	Geopolymer Concrete GC control beam without strengthening
<b>BF3</b>	GPC beam with single flat layer width 100 mm at tension face	<b>BS3</b>	GPC beam with single vertical U-shape layer strip width 150 mm
<b>BF4</b>	GPC beam with U-shape layer width 300 mm	<b>BS4</b>	GPC beam with two vertical U-shape layer strip width 50 mm
<b>BF5</b>	GPC beam with double flat layer width 100 mm at tension face	<b>BS5</b>	GPC beam with double vertical U-shape layer strip width 150 mm

### 2.3. Mixing and curing process

All tested specimens were cast in two groups (flexural and shear groups). Each group consists of five beams, six standard cubes, and three standard cylinders. All required materials were prepared at room temperature. Firstly, the wooden forms, cubes, and cylinders were cleaned and painted with oil to prevent concrete sticking, then the reinforcement steel was fixed in the wooden forms with a concrete cover for it. Fly ash, sand, and dolomite were placed in the mechanical mixer and mixed for about 2–3 min. After that the liquid solutions (Sodium hydroxide and sodium silicate) were added with additional mixing water to the mixture pan with continuous mixing for about 3 min to have the required workability. All specimens were poured in layers and vibrated on a laboratory vibration table for 10–15 s. Then they were left for 24 h in the wooden form after the end of the casting process, as shown in Fig. 8a. After that, all GPC specimens were removed from the wooden form as shown in Fig. 8b and c and cured in a dry oven at a temperature of 100 C for 24 h as shown in Fig. 8d, while RC specimens were cured by covering them with wet towels until the age of 28 days. Finally, GPC samples were removed and placed at room temperature for a total of 28 days.

### 2.4. Installation of carbon FRP sheets

The CFRP sheet, which is known commercially as SikaWrap® 230C, was cut to the required size as shown in Fig. 9a. The surfaces of the beam that would be strengthened were roughed and cleaned of dust, as shown in Fig. 9b. The sikadur® –330 was mixed to make the light grey component (resin part A: hardener part B = 4:1, respectively, by weight), then applied to the required surfaces of strengthening beams where CFRP sheets will be installed and pressed to remove inside voids and make sure that the sheet was fully saturated with resin as shown in Fig. 9c. Before testing, concrete strain gauges were installed at mid-span of the upper and lower surfaces for all beams after roughing it with sand to achieve coherence between gauges and concrete surfaces, as shown in Fig. 9d.

### 2.5. Testing setup

Initially, all beams were painted white to aid in the observation of crack propagation with necked eyes. The available hydraulic testing machine (Avery Denison-England, 1000 KN) was suitable based on the dimensions and span of the tested beams. The tested beam was installed on two roller supports with a clear span of 750 mm and 50 mm of free space on each side. The applied load of the

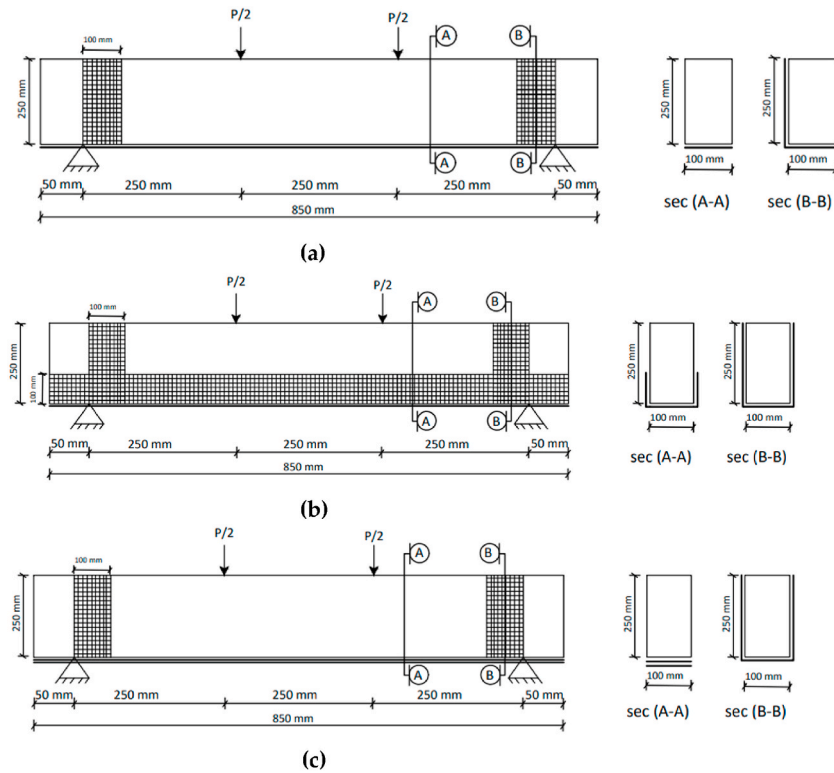


**Fig. 6.** Strengthening schemes with CFRP for flexural group. (a) Beam BF3 with single flat layer width 100 mm at tension face. (b) Beam BF4 with u-shape layer width 300 mm. (c) Beam BF5 with double flat layer width 100 mm at tension face.

hydraulic machine will be transmitted to the tested beam through a spreader beam or steel I-beam that is welded to two cylindrical rods from the bottom with 250 mm spacing between the two rods to ensure that the load is transmitted to the tested beam at two points (four-point loading according to ASTM C78), as shown in Fig. 10a. After that, the electrical strains and load cells were connected to the data logger to record load and strains, respectively. The LVDT was fixed at mid-span for all tested beams and connected to a data logger to measure deflection in mm. Finally, with the beginning of loading, the applied load will be transmitted to the tested beam through a steel I-beam to make the data logger start recording and storing readings. Fig. 10b shows a schematic for loading and set-up.

### 3. Results and discussions

The trial mixes of RC and GPC cubes and cylinders were tested at 28 days of age to make sure that all beams have achieved the required compressive and splitting tensile strengths. It was found that the average compressive strength of RC cubes was about 35.2 MPa, while it was about 37 MPa for GPC cubes. The splitting tensile strength of RC cylinders was about 2.42 MPa, and it was about 2.65 MPa for GPC.

#### 3.1. Flexural strengthening

Results were discussed and presented in terms of first cracking load, ultimate failure load, deflection at mid-span, longitudinal bar strain at mid-span and transverse stirrup strain at mid-shear span zone, concrete strain at top and bottom faces, crack pattern, and mode of failure for flexural group beams.

##### 3.1.1. The cracking, ultimate load and failure mode

As shown in Fig. 11(a–e), the flexural beams had failed under flexural mode of failure. For beams strengthened with CFRP sheets, the failure mode starts with small tension cracks at mid-span zone, then, yielding of steel followed by rupture of CFRP sheet, and crushing of the concrete at the compression zone. Table 7 shows the first cracking, yield, and ultimate load of flexural beams. It was observed that the first cracking load of the GPC control beam (BF2) is increased by 18% compared with (BF1). By using CFRP sheets, the first cracking loads were increased by about (20% & 32% and 24%) for strengthened beams (BF3 & BF4 and BF5) respectively, compared with (BF2). It was also observed that, the ultimate failure load of GPC control beam (BF2) has increased by 11% compared to RC control beam (BF1). By using CFRP sheets, the ultimate failure loads were increased by (10% & 16% and 19%) for strengthened beams (BF3 & BF4 and BF5) respectively. This indicated that, the various schemes of CFRP sheets have enhanced the failure load

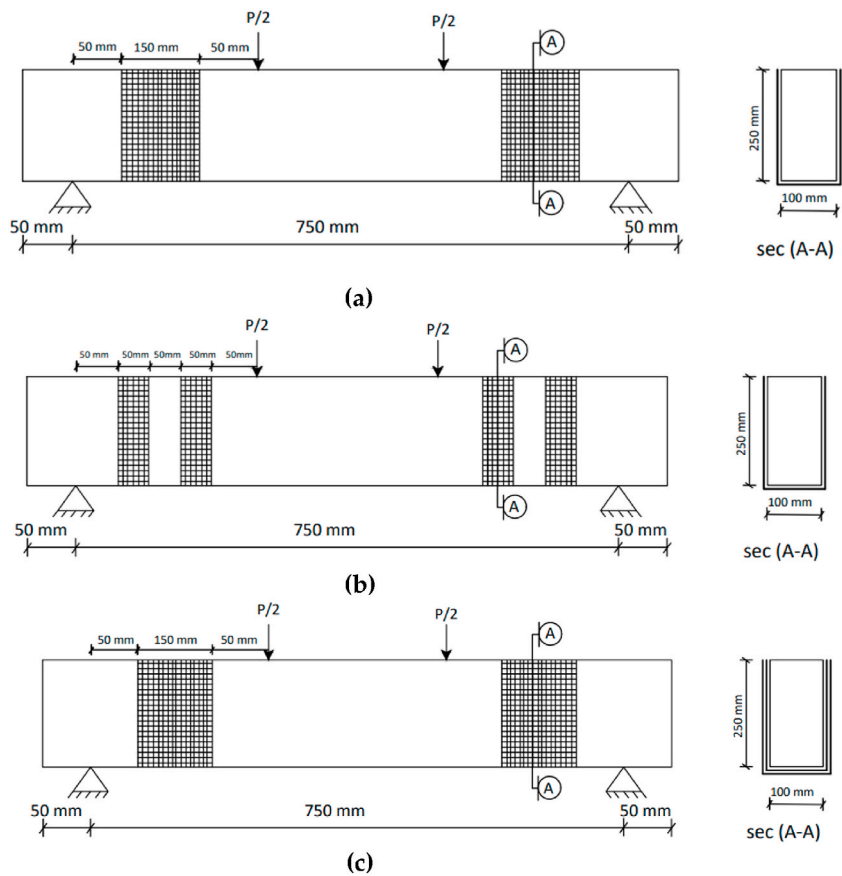


Fig. 7. Strengthening schemes with CFRP for shear group. (a) Beam BS3 with single vertical u-shape layer strip width 150 mm. (b) Beam BS4 with two vertical u-shape layer width 50 mm. (c) Beam BS5 with double vertical u-shape layer width 150 mm.

Table 5  
Mixing Proportions for 1m3 of RC and GPC beams.

Mixing proportions for 1m3 of RC control beams (Kg/m <sup>3</sup> )							
Sand Kg/m <sup>3</sup>	Dolomite Kg/m <sup>3</sup>	Extra water Kg/m <sup>3</sup>	Cement Kg/m <sup>3</sup>	Fly ash Kg/m <sup>3</sup>	Sodium Silicate Kg/m <sup>3</sup>	Sodium Hydroxide Kg/m <sup>3</sup>	Super plasticizer Kg/m <sup>3</sup>
650	4.7-10	10-15	190	400	-	-	-
Mixing proportions for 1m3 of GPC control and strengthening beams (Kg/m <sup>3</sup> )rowhead							
580	590	590	95	-	410	165	41
							8

capacity of flexural GPC beams and using double flat layer of CFRP at tension face is the best technique for improving the load capacity of GPC beams. The failure modes of Flexural group beams is presented in Fig. 11(a-e).

3.1.2. Load-deflection curves

As shown in Fig. 12, All tested beams have the same behaviour in linear and nonlinear stages especially for controls beams BF1 & BF2 while strengthened beams exhibited a higher post stiffness and increase in the first cracking, yield and ultimate load capacity as well as a significant decrease in deflection compared to control beams. The deflections were measured at mid-span of all tested beams and indicated that, under the same value of GPC Control beam Load at different stages, the deflection had decreased significantly for strengthened beams. As shown in Table 6 that, the deflection at yield load of GPC control beam BF2 has a lower value by 6% compared to R.C beam BF1, while strengthening beams with CFRP sheets it was decreased by (9% & 5% and 8%) for (BF3 & BF4 and BF5) respectively compared to GPC beam BF2 with about 7.33% decrease on average. Also it was found that, the ultimate failure deflection of the RC beam (BF1) equals 3.62 mm while the ultimate failure deflection of the GPC beam (BF2) equals 4.20 mm, and this shows that the ultimate failure deflection of the GPC has increased by 16% compared with the RC control beam BF1. By applying CFRP sheets, the deflection of strengthened beams has decreased by about (23%, 11%, and 16%) for beams BF3 & BF4 and BF5, respectively, compared to the GPC control beam BF2 with about 16.66% decrease on average. It was also observed that GPC beams strengthened with U-shape



**Fig. 8.** Casting and curing process for all specimens. (a) Beams immediately after casting. (b) GPC Beam after 24 h from casting. (c) Cubes specimens after 24 h from casting. (d) Curing of specimens in the dry oven.

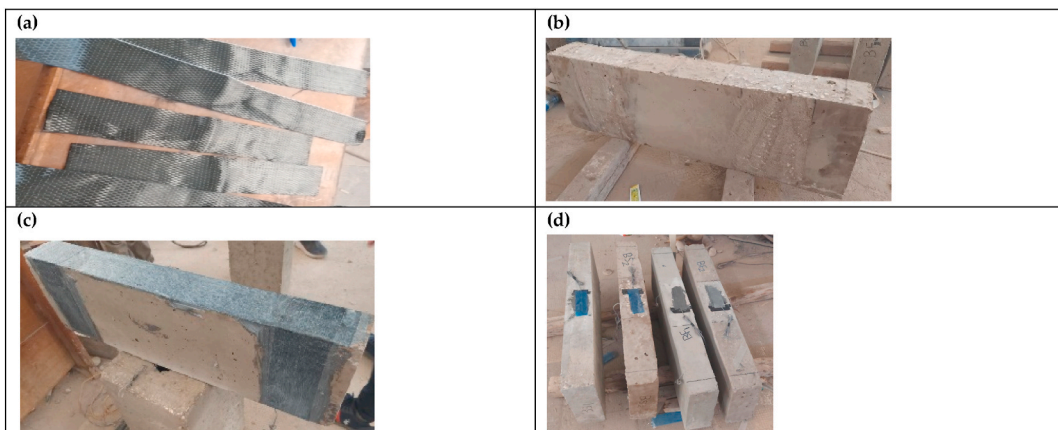


**Fig. 9.** Installation process of CFRP sheets. (a) Cutting the CFRP as the required size. (b) Roughing the concrete surface of tested beams. (c) Installation of CFRP with epoxy resin. (d) Concrete strain gauges for tested beams.

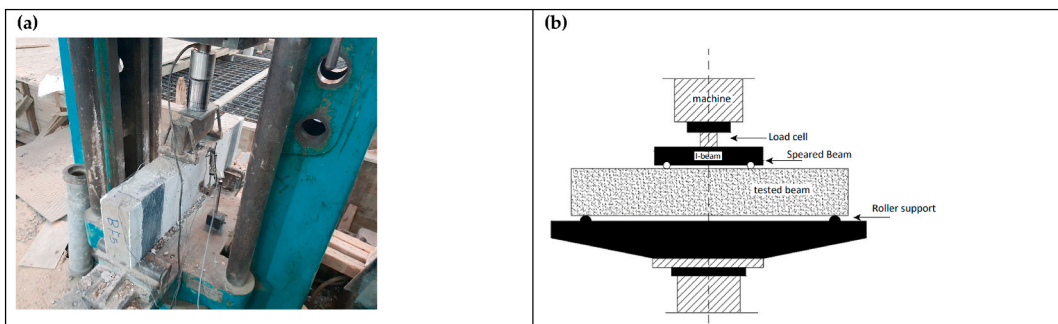


**Fig. 10.** Testing setup. (a) Loading Procedures for tested beams. (b) A schematic for loading and test set-up.



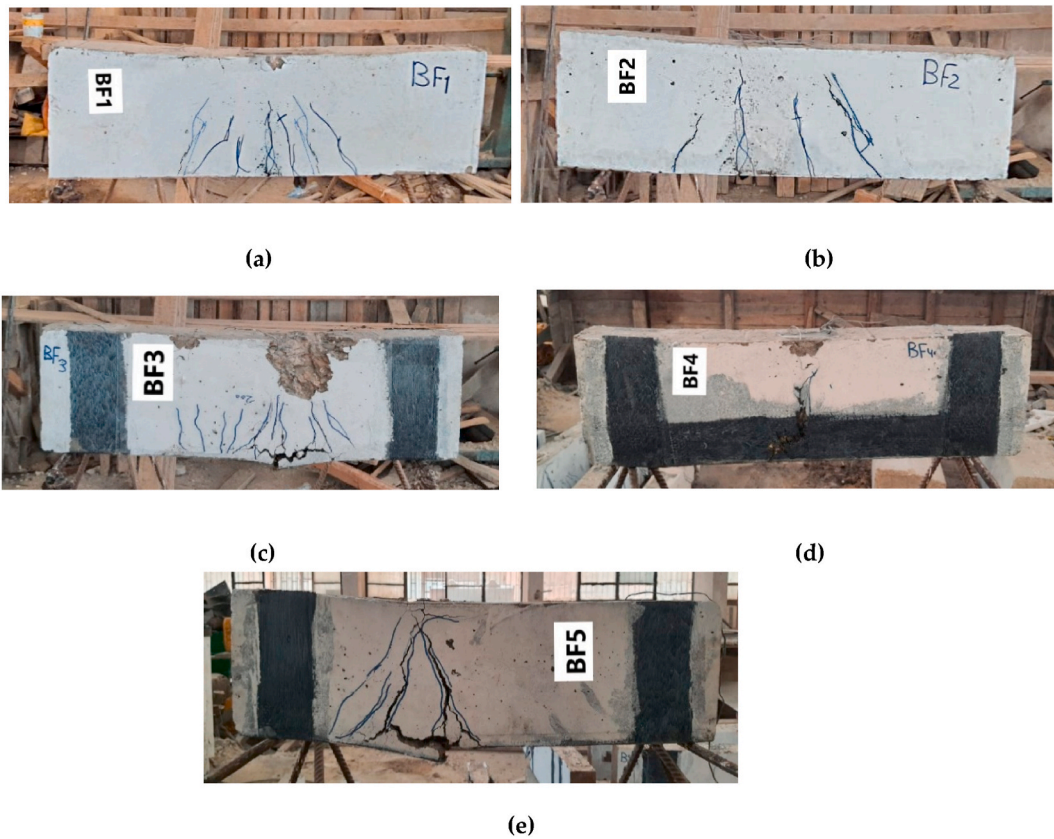


Fig. 11. Crack Pattern for Flexural group beams. (a) Crack Pattern for RC control beam BF1. (b) Crack Pattern for GPC control beam BF2. (c) Crack Pattern for strengthened GPC beam BF3. (d) Crack Pattern for strengthened GPC beam BF4. (e) Crack Pattern for strengthened GPC beam BF5.

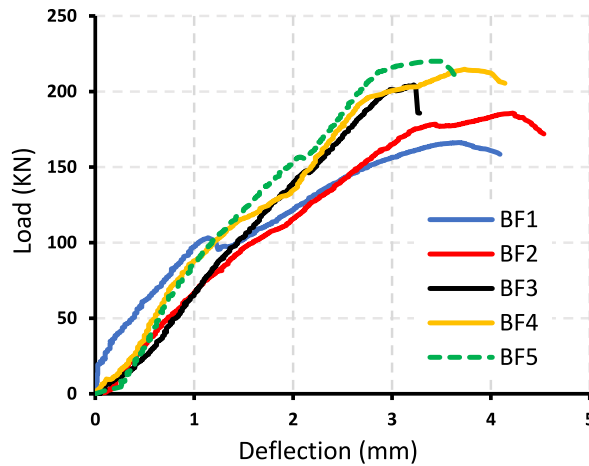


Fig. 12. Load-deflection curves for Flexural group beams.

layer BF4 and Double flat layers BF5 had stiffer behaviour when compared to control GPC beams.

### 3.1.3. Steel and concrete strains

As shown in Fig. 13a, the longitudinal bar strain of GPC control beam has increased slightly compared to RC beam. By using CFRP sheets, the longitudinal bar strains of strengthened GPC have decreased significantly at the same value of the applied load, and the same for transverse stirrup strain, as shown in Fig. 13b. For concrete strain, as shown in Fig. 13c & d, the concrete strain at top and bottom faces of GPC control beam has increased slightly compared to RC beam. By using CFRP sheets, the concrete strains of

**Table 6**  
Stiffness characteristic of Flexural group beams.

Beam Symbol	Pc (KN)	Pc/Pc*	Pu (KN)	Pu/Pu*	$\delta_c$ (mm)	$\delta_u$ (mm)	Pre-cracking Stiffness KN/mm	Post cracking Stiffness KN/mm	E.A1 KN.mm	E.A2 KN.mm
BF1	103	1.00	166	1.00	1.51	3.62	68.21	45.85	110	370
BF2	122	1.18	185	1.11	2.08	4.20	58.65	44.04	138	397
BF3	146	1.20	204	1.10	2.12	3.22	68.86	63.35	146	254
BF4	161	1.32	214	1.16	2.29	3.72	70.30	57.52	198	358
BF5	152	1.24	220	1.19	2.02	3.50	75.24	62.85	154	362

(pc, pu): Cracking and ultimate failure load.

(pc\*, pu\*): Cracking and ultimate failure load for GPC control beam (BF2).

E.A1, EA2: Pre and Post cracking energy absorption.

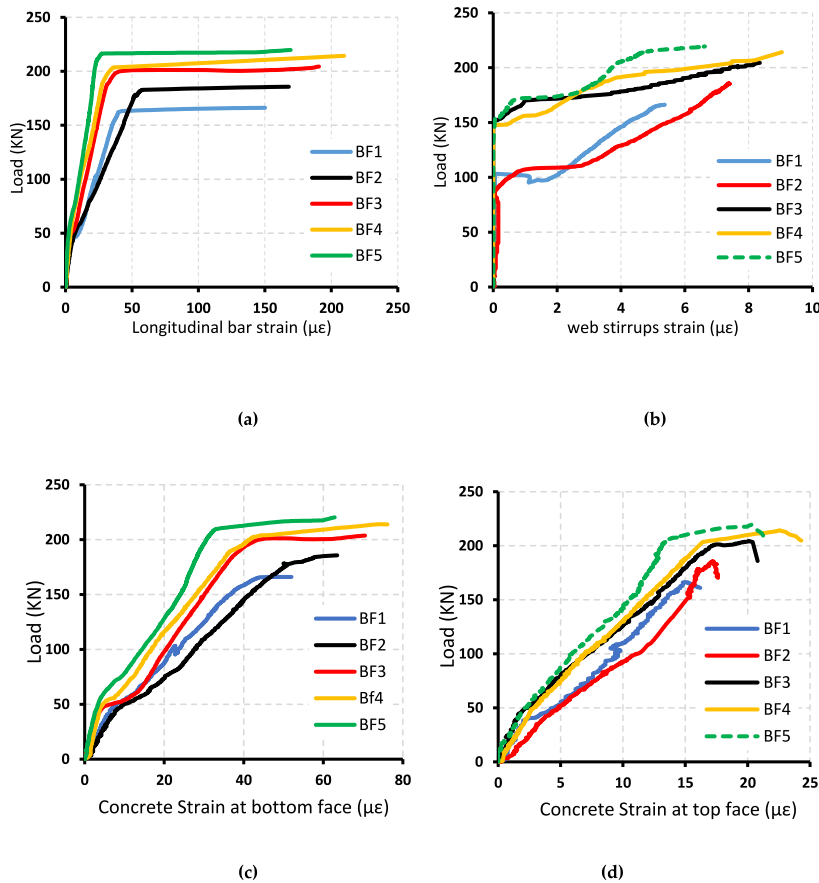


**Fig. 13.** Load verse steel and concrete strains for Flexural group beams. (a) Longitudinal bar strain at mid-span of flexural beams. (b) Stirrup strain at mid-shear span zone of flexural beams (c) concrete strain at bottom face of flexural beam. (d) concrete strain at top face of flexural beam.

strengthened GPC have decreased significantly at the same value of the applied load. Overall, flexural strengthening of GPC with CFRP sheets has proved its efficiency in decreasing steel and concrete strains.

**3.1.4. Stiffness and energy absorption**

As shown in Table 6, the experimental results indicated that, By using CFRP sheets, the first cracking loads were increased by about 25.33% on average while the ultimate failure loads were increased by about 15% on average compared to GPC control Beam (BF2). Also it was found that, the pre and post cracking stiffness of Strengthening GPC beams have increased by 21.8% and 39% on average respectively, compared to GPC beam BF2 and this prove the stiffer behavior of Strengthened GPC beams. The energy absorption is described as the area under the load mid span deflection curves, it was concluded that, the Pre cracking energy absorption of Strengthening GPC beams have increased by 20.36% on average compared to GPC control Beam BF2 while with the onset of CFRP sheet, the Post cracking energy absorption was decreased by 18.2% on average compared to GPC control Beam BF2. Overall, Flexural

Strengthening of GPC Beams with externally bounded CFRP sheets has proved it's efficiency for increasing Ultimate Failure Load and Stiffness as well as decreasing the Post Cracking energy absorption.

### 3.1.5. Ductility index and toughness

The ductility is described as the ratio of deflection at ultimate failure load to yield load. As shown in Table 7, the ductility index for RC beam (BF1) was 1.06, and the ductility of GPC control beam (BF2) was 1.31; this mean that, the ductility of GPC beam increased by 24% compared to (BF1). Strengthening GPC beams with CFRP sheets has remarkable effect on ductility as it was increased by (4% & 15% and 11%) for beams BF3 & BF4 and BF5 respectively compared to (BF1). As shown in Table 7, toughness of GPC beam (BF2) in flexural is increased by 11% compared to RC beam (BF1). By using the CFRP sheets, the toughness has decreased by 20% for (BF3) due to sudden rupture of CFRP sheet, but it has increased by (16% & 8%) for beams BF4 and BF5, respectively, compared to (BF1). This indicated that, GPC toughness in flexural is affected by strengthening system and increased with it.

## 3.2. Shear strengthening

Results are discussed and presented in terms of first cracking load, ultimate failure load, deflection at mid-span, longitudinal bar strain at mid span, concrete strain at top face, crack pattern, and mode of failure for shear group beams.

### 3.2.1. The cracking, ultimate load and failure mode

As shown in Fig. 14, all shear beams had failed under the shear mode of failure except for beam BS5, as it was strengthened enough to change the failure mode from shear to flexural with crushing of concrete at compression zone. For beams strengthened with CFRP strips, the failure mode starts with small and narrow diagonal shear cracks at shear span zone then, yielding of steel followed by rupture of CFRP strips until failure. Table 7 shows the first cracking, yield, and ultimate load of shear beams. It was found that, the first cracking load of GPC control beam (BS2) was increased by 44% compared with (BS1), While using CFRP strips the first cracking loads was increased by about (51% & 22% and 58%) for strengthened beams (BS3 & BS4 and BS5) respectively, compared to (BS2). It was found that the ultimate failure load of GPC beam (BS2) has increased by 23% compared to RC control beam (BS1). By using CFRP strips, the ultimate loads were increased by (57% & 69% and 79%) for strengthened beams (BS3 & BS4 and BS5) respectively. This indicated that, the various schemes of externally bound CFRP strips have enhanced the cracking and ultimate load capacity of shear GPC beams, and using double U-shape layer strips of CFRP is the best technique for improving the shear behavior of GPC beams. The failure mode for Shear group beams is presented in Fig. 14(a–e).

### 3.2.2. Load-deflection curves

The experimental results as shown in Fig. 15 indicated that, Control beams BS1 and & BS2 have a similar behavior in pre and post cracking stages while GPC strengthened beams had a significant higher stiffness. It was also noticed from Fig. 15 that, the various shemes of externally bonded CFRP strips at shear span zone has proved it's efficiency for increasing the first cracking, yield and ultimate failure load capacity as well as decreasing deflection copmared to control beams. Accordig to experimental results it was found that, the yield load of GPC control beam BS2 was equal 133 KN with a corresponding deflection of 2.36 mm and at the same load value, The deflections of strengthened beams BS3, BS4 and BS5 was equal (1.19,1.24 and 1.32 mm) respectively and this indicates that, the deflection of strengthened beams has decreased by about (49% & 47% and 44%) for BS3, BS4 and BS5 respectively compared to GPC control beam (BS2) with about 46.6% decrease on average. Also it was found that, The ultimate failure deflection for RC beam (BS1) equals 2.32 mm, while the ultimate failure deflection of GPC beam (BS2) equals 2.6 mm, and this shows that, the ultimate deflection of GPC has increased by 12% compared to RC control beam (BS1). As well as, using externally bonded CFRP strips increased the ultimate failure load, and therefore the ultimate deflection has increased to reach (3.29, 2.56 and 3.60 mm) for BS3, BS4 and BS5, respectively. The deflections of strengthened beams BS3, BS4 and BS5 was equal (1.82,1.56 and 1.71 mm) respectively, at the ultimate failure load value of GPC beam (BS2) and this indicates that, the deflection of strengthened beams has decreased by about (30% & 40% and 34%) for BS3, BS4 and BS5 respectively compared to GPC control beam (BS2) with about 34.6% decrease on average.

**Table 7**

Strength characteristic of Flexural group beams.

Beam Symbol	Pc (KN)	Pc/ Pc*	Py (KN)	Py/ Py*	Pu (KN)	Pu/ Pu*	$\delta y$ (mm)	$\delta y/\delta y^*$	$\delta u$ (mm)	$\delta u/\delta u^*$	$\delta u/\delta y$	Toughness KN. mm
BF1	103	1.00	164	1.00	166	1.00	3.40	1.00	3.62	1.00	1.06	480
BF2	122	1.18	177	1.08	185	1.11	3.20	0.94	4.20	1.16	1.31	535
BF3	146	1.20	198	1.12	204	1.10	2.92	0.91	3.22	0.77	1.10	400
BF4	161	1.32	202	1.14	214	1.16	3.05	0.95	3.72	0.88	1.22	556
BF5	152	1.24	212	1.20	220	1.19	2.96	0.92	3.50	0.83	1.18	516

(pc, py, pu): Cracking, yielding and ultimate failure load.

(pc\*, py\*, pu\*): Cracking, yielding and ultimate failure load for GPC control beam (BF2).

$\delta y$ ,  $\delta u$ : Deflection at yield and ultimate load.

$\delta u/\delta y$ : Ductility index.

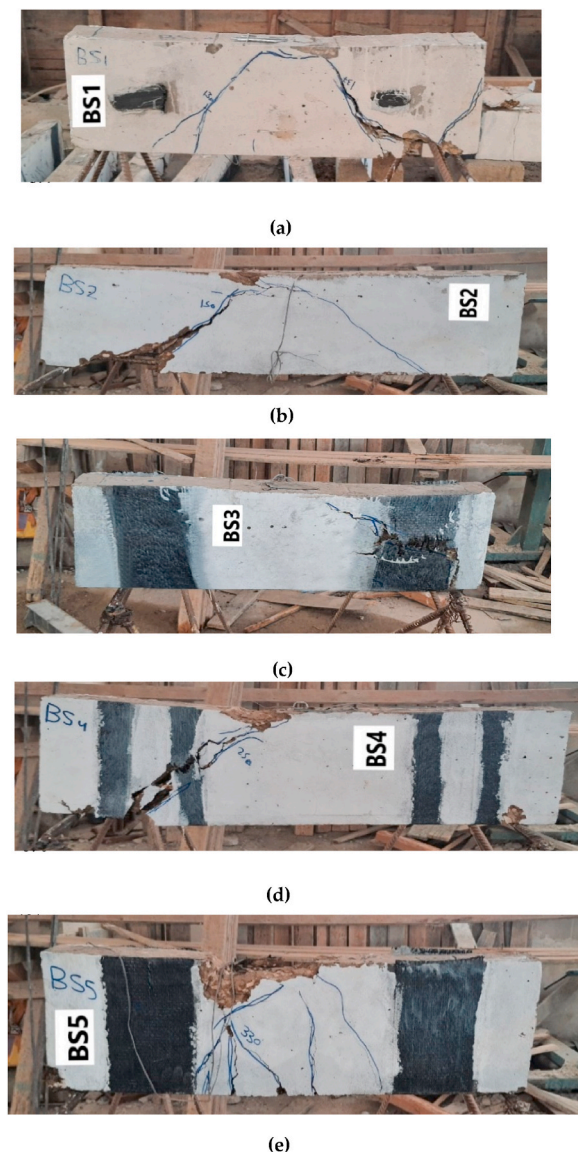


**Fig. 14.** Crack Pattern for Shear group beams. (a) Crack Pattern for RC control beam BS1. (b) Crack Pattern for GPC control beam BS2. (c) Crack Pattern for strengthened GPC beam BS3. (d) Crack Pattern for strengthened GPC beam BS4. (e) Crack Pattern for strengthened GPC beam BS5.

### 3.2.3. Steel and concrete strains

The longitudinal bar strain at mid span of as well as concrete strain at top face of shear tested beams were recorded, as shown in Fig. 16a & 16b. The longitudinal steel strain of GPC control beam (BS2) has increased slightly compared to RC beam (BS1). While using CFRP strips, it was greatly decreased at the same value of the applied load, as shown in Fig. 16a. For concrete strain as shown Fig. 16b, At the same value of applied load, the concrete strains at top faces of GPC and RC beam were almost similar. By using CFRP sheets, the concrete strains of strengthened GPC have slightly decreased at the same value of the applied load. Overall, shear strengthening of GPC with CFRP strips has proved its efficiency in decreasing concrete and steel strains.

### 3.2.4. Stiffness and energy absorption

The experimental results that shown in Table 8 indicated that, Using externally bounded CFRP strips has increased the first cracking loads and ultimate failure loads by 43% and 68% on average compared to GPC control Beam BS2. Also it was conducted that, Strengthening GPC beams with CFRP strips in shear has increased the pre and post cracking stiffness by 47.7% and 41% on average respectively, compared to GPC beam BS2 and this describe the stiffer behavior of Strengthened GPC beams. The Pre and Post cracking energy absorption was calculated to find that, shear Strengthening of GPC beams has increased slightly the Pre cracking energy absorption by 37.6% on average compared to GPC control Beam BF2 while the Post cracking energy absorption had increased highly by

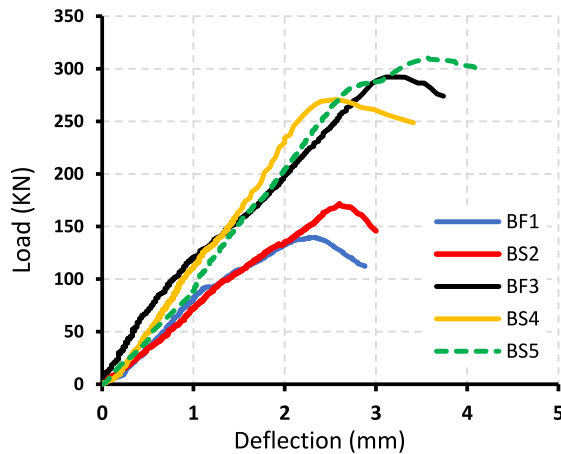


Fig. 15. Load -deflection curves for Shear group beams.

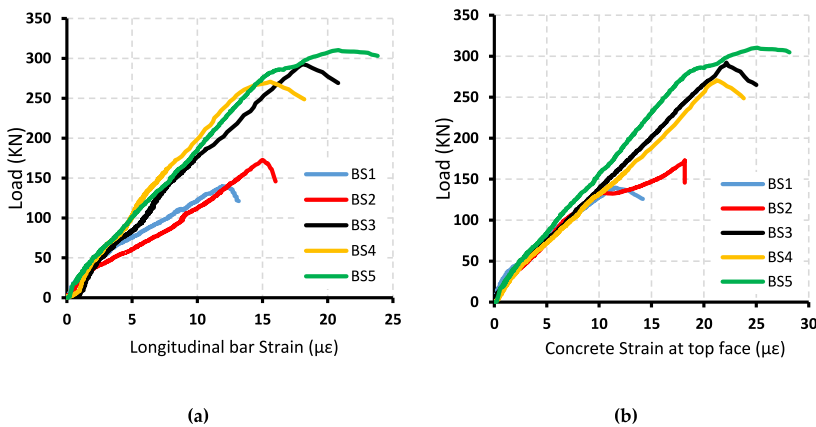


Fig. 16. Load verse steel and concrete strains for Shear group beams. (a) Longitudinal bar strain at mid-span of shear beams. (b) Concrete strain at top face of shear beam.

**Table 8**  
Stiffness characteristic of Shear group beams.

Beam Symbol	Pc (KN)	Pc/Pc*	Pu (KN)	Pu/Pu*	$\delta_c$ (mm)	$\delta_u$ (mm)	Pre-cracking Stiffness KN/mm	Post cracking Stiffness KN/mm	E.A1 KN.mm	E.A2 KN.mm
BS1	92	1.00	140	1.00	1.18	2.32	77.96	60.34	56	209
BS2	133	1.44	172	1.23	1.94	2.60	68.55	66.15	138	159
BS3	201	1.51	292	1.69	2.16	3.29	93.05	88.75	226	449
BS4	162	1.22	270	1.57	1.50	2.56	108	105.46	142	441
BS5	210	1.58	309	1.79	2.04	3.60	102.9	85.83	202	574

(pc, pu): Cracking and ultimate failure load.

(pc\*, pu\*): Cracking and ultimate failure load for GPC control beam (BS2) 182.3 1.77 261.

E.A1, EA2: Pre and Post cracking energy absorption.

206% on average compared to GPC control Beam BS2 as energy absorption has affected greatly by using CFRP strips which increased the ultimate load capacity by 68% on average. Overall, Various Schemes of externally bounded CFRP strips has proved it's efficiency for increasing Ultimate Failure Load, Stiffness and Cracking energy absorption.

### 3.2.5. Ductility index and toughness

As shown in Table 9, the ductility index of RC control beam (BS1) was 1.11 and that of GPC control beam (BS2) was 1.10 this means that, the ductility of GPC beam is almost similar to RC control beam (BS1). While using the CFRP strips, the ductility has increased by (9% & 5% and 12%) for beams BS3 & BS4 and BS5 respectively, compared to beam (BS1). As shown in Table 9, the toughness of GPC

**Table 9**  
Strength characteristic of Shear group beams.

Beam Symbol	Pc (KN)	Pc/ Pc*	Py (KN)	Py/ Py*	Pu (KN)	Pu/ Pu*	$\delta y$ (mm)	$\delta y$ / $\delta y^*$	$\delta u$ (mm)	$\delta u$ / $\delta u^*$	$\delta u$ / $\delta y$	Toughness KN. mm
BS1	92	1.00	134	1.00	140	1.00	2.09	1.00	2.32	1.00	1.11	265
BS2	133	1.44	156	1.16	172	1.23	2.36	1.13	2.60	1.12	1.10	297
BS3	201	1.51	265	1.69	292	1.69	2.72	1.15	3.29	1.26	1.21	675
BS4	162	1.22	250	1.60	270	1.57	2.21	0.94	2.56	0.98	1.16	583
BS5	210	1.58	286	1.83	309	1.79	2.9	1.23	3.60	1.53	1.24	776

(pc, py, pu): Cracking, yielding and ultimate failure load.

(pc\*, py\*, pu\*): Cracking, yielding and ultimate failure load for GPC control beam (BS2).

$\delta y$ ,  $\delta u$ : Deflection at yield and ultimate load.

$\delta u/\delta y$ : Ductility index.

beam in shear (BS2) is increased by 12% compared to RC control beam (BS1). The toughness has affected greatly by using CFRP strips as it was increased (255% & 220% and 292%) for BS3 & BS4 and BS5 respectively compared to (BS1) due to the CFRP strips has increased the ultimate load capacity by 68% on average and flexural failure mode of (BS5). This means that, shear strengthening of GPC beams with different schemes of externally bound CFRP strips has worked efficiently for increasing GPC toughness, respectively, compared to (BS1). As shown in Table 9, the toughness of GPC beam in shear (BS2) is increased by 12% compared to RC control beam (BS1). The toughness has affected greatly by using CFRP strips as it was increased (255% & 220% and 292%) for BS3 & BS4 and BS5 respectively compared to (BS1) due to the CFRP strips has increased the ultimate load capacity by 68% on average and flexural failure mode of (BS5). This meant that, shear strengthening of GPC beams with different schemes of externally bound CFRP strips had worked efficiently for increasing GPC toughness.

#### 4. Conclusions

The objective of this experimental study is to investigate the structural response (shear and flexural) of GPC beams strengthened with CFRP sheets. A set of ten tested beams with the same cross section were carried out and tested up to failure under two symmetric static loading. Depending on the experimental results presented in this research, the following conclusions are drawn:

1. The mid-span deflection for flexural GPC beams strengthened with (single flat layer & u-shape single layer and double flat layer) of CFRP sheets had decreased by (23% & 11% and 16%) respectively, with about 16% an average decrease in deflection.
2. The first cracking load of flexural strengthening GPC beam with (single flat layer & u-shape single layer and double flat layer) of CFRP sheets had increased by (20% & 32% and 24%) respectively, with about 25.33% an average increase in first cracking load.
3. The yield load of flexural strengthening GPC beam with (single flat layer & u-shape single layer and double flat layer) of CFRP sheets had increased by (12% & 14% and 20%) respectively, while the ultimate failure load had increased by (10% & 16% and 19%) respectively.
4. The Flexural behavior of strengthened GPC beams exhibited a higher stiffness in pre and post cracking stages and increased by 21.8% and 39% on average respectively compared to control GPC beams BF2.
5. The flexural ductility of GPC beams had increased by 24% compared to RC control beam. By using various strengthening schemes of CFRP sheets, it has improved and increased by 10% on average compared to RC beam.
6. The flexural toughness of GPC beam had increased by 11% compared to RC control beam. By using the CFRP sheets, the toughness has increased by 12% on average compared to RC beam.
7. The mid span deflection of shear GPC beams had increased by 12% compared to RC control beam. By using (single u-shape layer & two u-shape layers and double u-shape layer) of CFRP strips, the deflection had decreased by (30% & 40% and 34%) respectively, at the same value of the ultimate load for GPC control beam.
8. The shear first cracking load for GPC beam with (single u-shape layer & two u-shape layer and double u-shape layer) of CFRP strips had increased by (51% & 22% and 58%) respectively, while the yield load had increased by (69% & 60% and 83%) respectively.
9. The shear ultimate load for GPC beam strengthening with (single u-shape layer & two u-shape layer and double u-shape layer) of CFRP strips had increased by (69% & 57% and 79%) respectively, with about 68 %an average increase in ultimate failure load.
10. The shear ductility of GPC beams is almost similar to RC control beam. While using CFRP strips, it has increased by 8% on average compared to RC beam.
11. The Shear behavior of strengthened GPC beams has a significant increasing in the pre and post cracking stiffness by 47.7% and 41% on average respectively, compared to GPC beam BS2.

#### Funding

“This research received no external funding”.

## Author contribution statement

Ahmed S. EISA, Dr.; Mostafa H. AHMED, Dr: Conceived and designed the experiments; Performed the experiments; Analyzed and interpreted the data; Contributed reagents, materials, analysis tools or data; Wrote the paper.

Ivo DEMJAN, Dr.: Analyzed and interpreted the data; Contributed reagents, materials, analysis tools or data.

Dušan Katunský, PhD.: Analyzed and interpreted the data; Contributed reagents, materials, analysis tools or data; Wrote the paper.

## Data availability statement

Data included in article/supp. material/referenced in article.

## Declaration of competing interest

The authors declare that they have no known competing financial interests or personal relationships that could have appeared to influence the work reported in this paper.

## References

- [1] N. Singh, B. Middendorf, Geopolymers as an alternative to Portland cement: an overview, *Construct. Build. Mater.* 237 (2020), 117455.
- [2] A.G. Alex, et al., Flexural behavior of low calcium fly ash based geopolymer reinforced concrete beam, *International Journal of Concrete Structures and Materials* 16 (1) (2022) 1–11.
- [3] A.L. Almutairi, et al., Potential applications of geopolymer concrete in construction: a review, *Case Stud. Constr. Mater.* 15 (2021), e00733.
- [4] C.R. Meesala, N.K. Verma, S. Kumar, Critical review on fly-ash based geopolymer concrete, *Struct. Concr.* 21 (3) (2020) 1013–1028.
- [5] S.V. Patankar, Y.M. Ghugal, S.S. Jamkar, Mix design of fly ash based geopolymer concrete, in: *Advances in Structural Engineering*, Springer, 2015, pp. 1619–1634.
- [6] R. McCaffrey, Climate change and the cement industry, *Global cement and lime magazine (environmental special issue)* 15 (2002) 19.
- [7] K. Vijai, R. Kumutha, B. Vishnuram, Effect of types of curing on strength of geopolymer concrete, *Int. J. Phys. Sci.* 5 (9) (2010) 1419–1423.
- [8] R.M. Andrew, Global CO<sub>2</sub> emissions from cement production, 1928–2018, *Earth Syst. Sci. Data* 11 (4) (2019) 1675–1710.
- [9] S. Luhar, I. Luhar, Additive manufacturing in the geopolymer construction technology: a review, *Open Construct. Build Technol. J.* 14 (1) (2020).
- [10] A. Hassan, M. Arif, M. Shariq, Use of geopolymer concrete for a cleaner and sustainable environment—A review of mechanical properties and microstructure, *J. Clean. Prod.* 223 (2019) 704–728.
- [11] J. Davidovits, Geopolymers: man-made rock geosynthesis and the resulting development of very early high strength cement, *J. Mater. Educ.* 16 (1994), 91–91.
- [12] N. Van Chanh, B.D. Trung, D. Van Tuan, Recent research geopolymer concrete, in: *The 3rd ACF International Conference, ACF/VCA, Vietnam, 2008*.
- [13] T. Luukkonen, et al., One-part alkali-activated materials: a review, *Cement Concr. Res.* 103 (2018) 21–34.
- [14] N. Lloyd, V. Rangan, Geopolymer concrete with fly ash, in: *Proceedings of the Second International Conference on Sustainable Construction Materials and Technologies*, UWM Center for By-Products Utilization, 2010.
- [15] F.N. Okoye, S. Prakash, N.B. Singh, Durability of fly ash based geopolymer concrete in the presence of silica fume, *J. Clean. Prod.* 149 (2017) 1062–1067.
- [16] P. Pradhan, et al., Durability characteristics of geopolymer concrete - progress and perspectives, *J. Build. Eng.* 59 (2022), 105100.
- [17] B. Singh, et al., Geopolymer concrete: a review of some recent developments, *Construct. Build. Mater.* 85 (2015) 78–90.
- [18] J.L. Provis, J.S.J. Van Deventer, *Geopolymers: Structures, Processing, Properties and Industrial Applications*, Elsevier, 2009.
- [19] M.B. Karakoc, et al., Sulfate resistance of ferrochrome slag based geopolymer concrete, *Ceram. Int.* 42 (1) (2016) 1254–1260.
- [20] Y. Wu, et al., Geopolymer, green alkali activated cementitious material: synthesis, applications and challenges, *Construct. Build. Mater.* 224 (2019) 930–949.
- [21] Z. Li, Z. Ding, Y. Zhang, Development of sustainable cementitious materials, in: *Proceedings of International Workshop on Sustainable Development and concrete technology*, Beijing, China, 2004.
- [22] S. Wallah, B.V. Rangan, *Low-calcium Fly Ash-Based Geopolymer Concrete: Long-Term Properties*, 2006.
- [23] J.R. Yost, et al., Structural behavior of alkali activated fly ash concrete. Part 2: structural testing and experimental findings, *Mater. Struct.* 46 (3) (2013) 449–462.
- [24] A. Hutagi, R.B. Khadiranaikar, Flexural behavior of reinforced geopolymer concrete beams, in: *International Conference on Electrical, Electronics, and Optimization Techniques, ICEEOT*, 2016, 2016.
- [25] Sharmila, S., K. Nalinaa, and N. Rajmane, *Effect of Shear Span on the Behaviour of Shear Critical Reinforced Geopolymer Concrete Beams—An Analytical Study*.
- [26] E.H. Chang, *Shear and Bond Behaviour of Reinforced Fly Ash-Based Geopolymer Concrete Beams*, Curtin University, 2009.
- [27] N.S. Yacob, et al., Shear strength of fly ash-based geopolymer reinforced concrete beams, *Eng. Struct.* 196 (2019), 109298.
- [28] S. Fareed, Behaviour of reinforced concrete beams strengthened by CFRP wraps with and without end anchorages, *Procedia Eng.* 77 (2014) 123–130.
- [29] R.P. Sherwin, et al., Flexural behaviour of geopolymer RC beams using CFRP sheet, *Int. J. Appl. Eng. Res.* 10 (51) (2015).
- [30] Sika Fly Ash® Concrete Additive, Available Online: <https://egy.sika.com/content/dam/dms/egy01/e/Sika%20Fly%20Ash.pdf>.
- [31] *ASTM C618-19*, Standard Specification for Coal Fly Ash and Raw or Calcined Natural Pozzolan for Use in Concrete, ASTM International, West Conshohocken, PA, USA, 2019.
- [32] A.M. Fernandez-Jimenez, A. Palomo, C. Lopez-Hombrados, Engineering properties of alkali-activated fly ash concrete, *ACI Mater. J.* 103 (2) (2006) 106.
- [33] J. Wongpa, et al., Compressive strength, modulus of elasticity, and water permeability of inorganic polymer concrete, *Mater. Des.* 31 (10) (2010) 4748–4754.
- [34] B. Joseph, G. Mathew, Influence of aggregate content on the behavior of fly ash based geopolymer concrete, *Sci. Iran.* 19 (5) (2012) 1188–1194.
- [35] *ASTM C109*, Standard Test Method for Compressive Strength of Cylindrical Concrete Specimens, ASTM International, West Conshohocken, PA, USA, 2021.
- [36] *ASTM C496/C496M-17*, Standard Test Method for Splitting Tensile Strength of Cylindrical Concrete Specimens, ASTM International, West Conshohocken, PA, USA, 2017.